| BULETINUL<br>Universităţii Petrol – Gaze din Ploieşti | Vol. LXVI<br>No. 4/2014 | 17 - 26 | Seria Tehnică |
|---|---|---|---|

# The Crack Growth as a Function of Loading Cycle's Number, Established by Two Experimental Methods

Viorel Goanţă, Marian Mareş, Bogdan Leiţoiu

Universitatea Tehnică "Gheorghe Asachi", Bd. Mangeron, 57, Iaşi
e-mail: vgoanta@tuiasi.ro

## Abstract

*Two experimental methods are described, used for studying the crack length increase, in dependence with the loading cycle's number. The basis for both methods is the tension test, applied on compact specimens of annealed OLC45 carbon steel. The first technique is using the specialized software on the computer of the testing machine, in order to establish the crack length propagation, by collecting the data from the machine loading cell, and also from the clip-on-gage extensometer that is attached on the compact specimen. For the second method, the experimental data on the crack length propagation are supplied by a dedicated crack propagation gage, provided by Vishay (Tk-09-CPB02-005/DP) and bonded in the vicinity of the initial small crack, initiated by fatigue. Finally, a comparison of the results obtained with the two methods is made; one can say that the advantage of the second method consists in its amenability for studying the crack growth rate on a real component, even without interrupting its working process.*

**Key words:** *crack growth, cyclic loading, crack propagation gage.*

## The Modeling of Fatigue Crack Initiation and Propagation

When a cycling load of a metallic component becomes stable, it could produce plastic strains, together with continuous transformations into the material structure, given by the presence of dislocations and the possibility of their movement during the loading. Many types of calculus relationship (possible empirical, in a measure) could be used, in order to estimate the necessary number of loading cycles for the fatigue crack initiation [1]. Such a formula is based on the local strains amplitude, in the vicinity of the initiation region [2]:

$$\log N_i = C^* + D \log \sqrt{E \sigma_{max} \varepsilon_{max}} \tag{1}$$

where $C^*$ and $D$ are assumed as material parameters, $E$ is its Young modulus, $\sigma_{max}$ – the maximum stress at the crack tip, and $\varepsilon_{max}$ – the local strain amplitude, on the loading direction.

Another method was described [3, 4], for a crack with a basis radius $\rho$=2 mm, in a part made of steel with 0.2% C content; the $N_i$ number, of loading cycles leading to 0.1 mm of crack propagation, may be obtained from the following formula:

$$\log k_N = 1{,}2969 - 0{,}1602 \log N_i \tag{2}$$

having the Neuber's coefficient defined as:

$$k_N = 1 + \frac{\alpha_t - 1}{1 + \sqrt{\dfrac{q}{\rho}}} \tag{3}$$

where $q$ is another material parameter (equal with 0.32 for a soft steel), and $\alpha_t$ – the theoretical coefficient of stress concentration, for the given loading state.

The recently developed methods are based on the stress intensity factor, as the evaluation parameter for estimating the necessary loading cycle's number, in order to initiate the fatigue crack. In this regard, for a soft steel prismatic specimen, having 20 mm in width and 5 mm in thickness, in which a sharp crack ($\rho < 0.2$ mm) is made, the $N_i$ number, of loading cycles leading to 0.1 mm of crack propagation is:

$$N_i = \frac{2{,}9 \cdot 10^8}{(\Delta K)^4} \tag{4}$$

A multitude of calculus relations, but also of theories and models were proposed, for the estimation of the crack propagation rate; their applicability is usually restricted, because they are not available for all the three domains that are described in Figure 1.

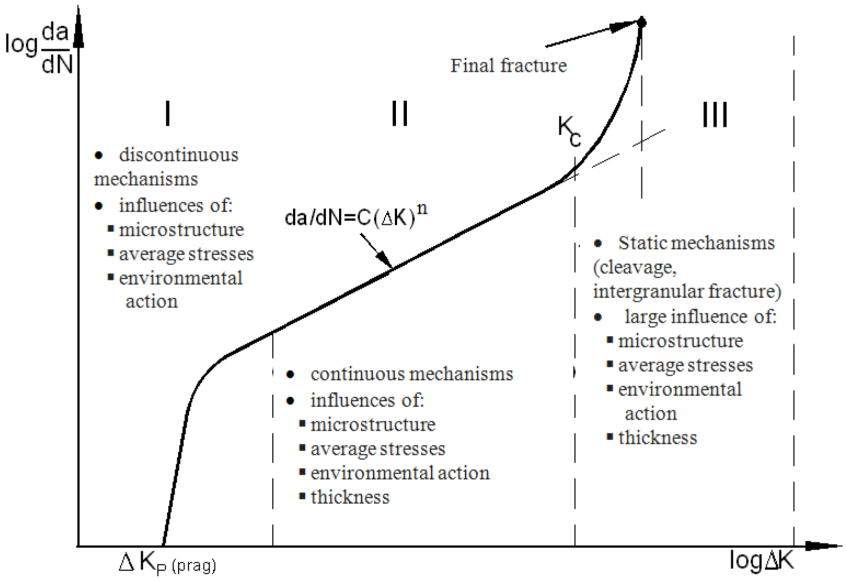

**Fig. 1**. The variation of crack propagation rate, as a function of the variation of the stress intensity factor.

The following presented calculus relations are the most frequently used for design purposes.

1. *The Paris law* is the mathematical expression (in logarithmic coordinates) of the linear variation (the second domain in figure 1) of the crack propagation rate, in dependence with the stress intensity factor [5], as:

$$\frac{da}{aN} = C(\Delta K)^n \tag{5}$$

   The constant values $C$ and $n$ must be experimentally established, being influenced by the material microstructure, environmental conditions, loading type and the asymmetry coefficient of loading cycle. The value of $n = 4$ was proposed by Paris, for the curve slope on the second domain of the cited graph. As a result of numerous experimental researches, the values of $n$ were established between 2 and 7, for most ductile materials, with the major values corresponding to brittle materials.

2. *The Donahue's relation* [6]:

$$\frac{da}{aN} = C(\Delta K - \Delta K_p)^n \tag{6}$$

was proposed for some little variations ΔK (the first domain in figure 1), and $\Delta K_p$ is the limit value of ΔK parameter, calculated with the Klesnil-Lucas formula [7]:

$$\Delta K_p = (1-R)^{\gamma}\,\Delta K_{p0} \tag{7}$$

The limit value $\Delta K_{p0}$ is obtained for $R = 0$, and $\gamma$ is a material parameter.

3. *The Weertman's relation* is a semi-empirical one [8], and it is used for the dependence of the second and the third domains in Figure 1, as:

$$\frac{da}{dN} = C\frac{\Delta K^4}{K_c^2 - K_{max}^2} \tag{8}$$

4. *The generalized relations.* The experimental data were shown, for many materials and loading situations, the three domains in Figure 1 are united in one alone. Some different mathematical functions were proposed, as a consequence, for describing the entire dependence curve from above, d*a*/d*N*=*f*(Δ*K*). In this regard, the *Austen's* relation (recommended for civil engineering steels) may be firstly cited as [9]:

$$\frac{da}{dN} = \frac{\Delta K^2}{4\pi\sigma_c E}\sqrt{\left(\frac{\Delta K - \Delta K_p}{K_{Ic} - \dfrac{\Delta K}{1-R}}\right)} \tag{9}$$

Another calculus relation was proposed by Erdogan and Ratwani [10] as:

$$\frac{da}{dN} = \frac{C(1+\beta)^n \Delta K^{n_1}\left(\Delta K - \Delta K_p\right)^{n_1}}{K_c - (1+\beta)\Delta K} \tag{10}$$

where *C, n* and $n_1$ are material parameters, and $\beta$ is given by the formula:

$$\beta = \frac{K_{max} + K_{min}}{K_{max} - K_{min}}$$

The $(1+\beta)^n$ factor is presumed to consider the medium stress influence on the fatigue crack propagation; the expression from the fraction denominator corresponds to the experimental data that are obtained from high level of loading stress. By contrast, the $\left(\Delta K - \Delta K_p\right)^{n_1}$ factor is considering the low levels of loading stress, together with the $\Delta K_p$ limit level. When appropriate values are available for the material parameters, a good correlation is obtained, for the results from Eq. (10), with the experimental data, for a crack propagation rate between $25\cdot 10^{-8}$ and 0.25 mm/cycle.

## The Use of Crack Propagation Gages for the Crack Growth Study

Such a transducer is based on a printed filament grating, fine and brittle, that is bonded on the material surface, at the crack tip, as it can be seen in Figure 2. When the crack is propagating, the grating elements are successively broken, and the electrical resistance that is measured between the A and B points increases. The resistance variation is indicated by a P3 (Vishay) Wheatstone bridge (being equipped with recording and storage data capabilities), and it is correlated with the transducer dimensions, in order to establish the crack length propagation. A range of crack propagation gage is produced and marketed by Vishay Intertechnology, Inc. [11]. The present experiment is using the model TK-09-CPB02-005, having a narrow grating and some specific characteristics, as presented in Figure 2.

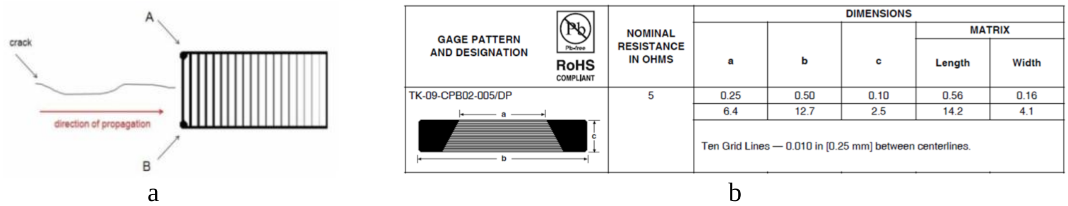

| GAGE PATTERN AND DESIGNATION | RoHS COMPLIANT | NOMINAL RESISTANCE IN OHMS | DIMENSIONS a | b | c | MATRIX Length | Width |
|---|---|---|---|---|---|---|---|
| TK-09-CPB02-005/DP | | 5 | 0.25 | 0.50 | 0.10 | 0.56 | 0.16 |
| | | | 6.4 | 12.7 | 2.5 | 14.2 | 4.1 |
| | | | Ten Grid Lines — 0.010 in [0.25 mm] between centerlines. | | | | |

**Fig. 2.** The principle and the real aspect of a crack propagation gage for measuring the crack propagation: the electrical resistance is measured between A and B points [12].

Such a sensor is able to measure up to ten steps of a crack increase, with the ten breakable elements of the grating, placed at a distance of 0.25 mm each. The grating steps have an increasing electrical resistance, and so the grating total resistance has a non-linear variation, in dependence with the number of broken filaments (see the diagram from figure 3).

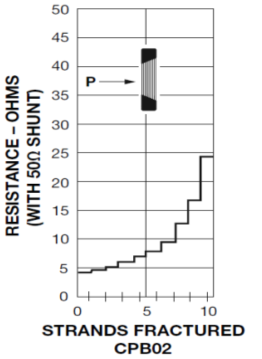

**Fig. 3.** Electrical resistance variation of the crack propagation gage, when the grating filaments are successively broken.

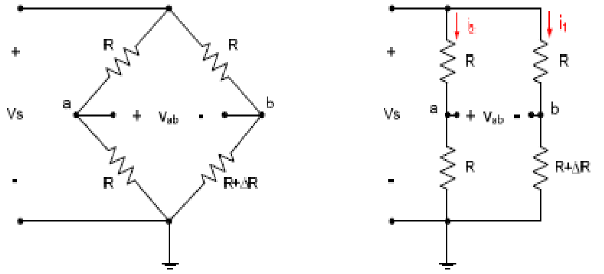

**Fig. 4.** The P3 bridge connection, in order to measure the electrical resistance variation of the crack propagation gage.

Into the non-balanced state, only the step-by-step resistance increments are indicated by the P3 bridge, and using the constant loading frequency, the cycle loading number between the breakage of two successive filaments can be calculated.

The Wheatstone bridge (see figure 4, together with the electrical connection that is presented in figure 5) is converting a ΔR electrical variation into a voltage variation $V_{ab}$, that is read on the measuring diagonal of the electric circuit, when a constant voltage $V_s$ is applied on its supplying diagonal.

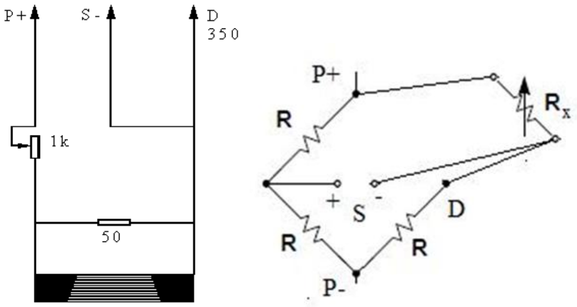

**Fig. 5.** The electrical circuit used for connecting the crack propagation gage with the P3 bridge: the P+, S- and D 350 quotations are indicating the bridge connectors, for a quarter-bridge model.

Assuming an equal electrical resistance for each of the bridge arms, the voltage on the measuring diagonal can be calculated as:

$$V_{ab} \cong -\frac{\Delta R}{4R} V_S \tag{11}$$

As a consequence, an electrical voltage of

$$V_0 \cong -\frac{\Delta R}{4R} V_{in}$$

is processed by the P3 bridge, and then displayed as a strain value (με), for every step of filament breakage. The 1kΩ potentiometer is used for adjusting the equivalent resistance of the active bridge arm ($R_x$, between the P+ and D points), leading for the starting indication to be situated close to the lower level of the displaying range (-30000με); the step-by-step filament breakage leads to an electrical resistance increase, and a corresponding increase of the strain value, up to the upper limit level of +30000με.

The stored data, from the bridge memory, could afterwards be processed, having in view the crack growth in dependence with loading cycle number, as indicated by the increasing strain values corresponding to the step-by-step breakage of the crack propagation gage filaments.

## The Testing Program

The "d*a*/d*N*" experimental program, for measuring the crack propagation rate, is based on a fatigue tensile test, conducted on carbon steel OLC 45 compact (CT) specimens (see figure 6) having each a lateral small notch (also obtained by some initial fatigue tests) that is acting as a stress-concentrator [13]. As a result of the variable loading that is applied on the notched specimen, the respective crack tends to increase, starting at the notch tip, and having the appearance of the real components cracks. The crack length is recorded, in dependence with the corresponding number of loading cycles, and the experimental data are processed, in order to establish the rate of crack propagation; that characteristic value is expressed as a function of the stress intensity factor at the crack tip Delta-K (Δ*K*), which is calculated on the basis of the linear-elastic analysis.

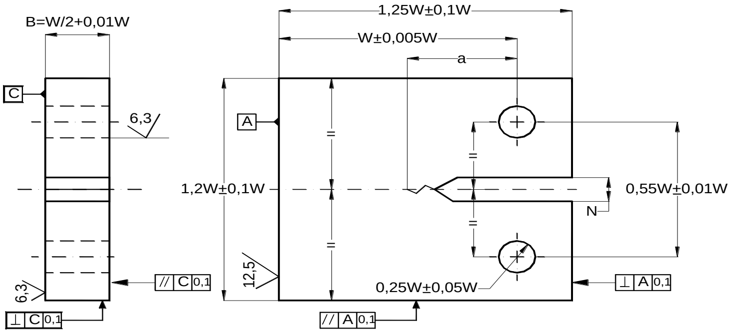

**Fig. 6.** The CT (compact tension) specimen

The specimen that is tested with the above described experimental technique could have any values of thickness and strength, but they must thick enough for preventing their buckling, or the appearance of plastic strains. The method may be used on specimens having a large range of proportional dimensions, but appropriate specimen dimensions could be chosen, for a specific test program, in dependence with the values of the applied load, and of the yield strength of the tested material. The crack length propagation is visually observed, in most cases, but it could be also established using some other methods, based on the potential difference, or the compliance measure at the unload stage. On the other hand, the experimental program for measuring the crack propagation rate was established according the basic principles of ASTM Standard E647 [14]. The testing parameters are introduced into the main data display, and the program principal menu is completed with data regarding the lot of specimens, the configuration and dimensions of the proper specimen, and some other testing and control parameters. All these data are recorded as a unique, personalized testing configuration, being available for using in similar or identical later experiments. During the tests, a graph is displayed, indicating the wave aspect of the applied variable load; another graph on the display is giving the crack length, as a function of cycles number, or the loading force, in dependence with the output signal of the extensometer (COD), or some other variation graph, that could be chosen from the program menu.

The program could also use the compliance method, for calculating the crack length increase; the mathematical relation between the compliance and the crack length was initially established, analytically, using a certain number of standard specimens, including the compact one (CT). In these equations the compliance is usually expressed in non-dimensional terms, as:

$$U = \frac{1}{\sqrt{\frac{E\nu B_{eff}}{F}} + 1} \tag{12}$$

using the normalized crack length, $a/W$, which is defined as:

$$\frac{a}{W} = \sum_{i=0}^{5}\left(C_i U^i\right) \tag{13}$$

The symbols in the above equations are: $E$ – the studied material Young's modulus; $v$ and $F$ – the displacement and the force between the measuring points; $W$ and $B_{eff}$ – the specimen width and effective thickness; $a$ – the crack length; $C_i$ – the compliance coefficients that are presented in Table 1 [13].

**Table 1**. Specific compliance coefficients values for the compact specimen CT

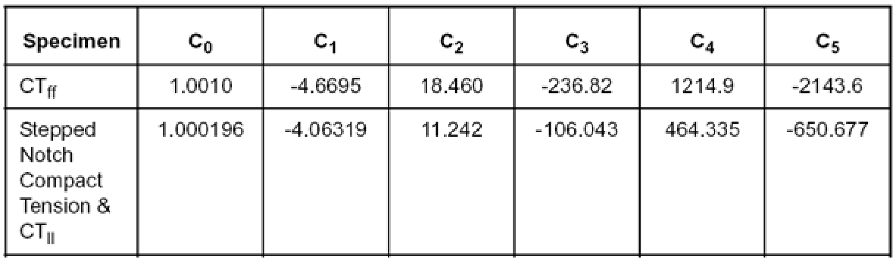

| Specimen | $C_0$ | $C_1$ | $C_2$ | $C_3$ | $C_4$ | $C_5$ |
|---|---|---|---|---|---|---|
| $CT_{ff}$ | 1.0010 | -4.6695 | 18.460 | -236.82 | 1214.9 | -2143.6 |
| Stepped Notch Compact Tension & $CT_{ll}$ | 1.000196 | -4.06319 | 11.242 | -106.043 | 464.335 | -650.677 |

For the compact specimen (CT), the coefficients are referring both at the frontal surface and, respectively, at the loading points of the specimen (in dependence with the measuring points of the displacement v – with the extensometer on the frontal surface, or by displacing the traverse of the testing machine at the points where the load is applied). The experimental results from the above described testing program are used for observing the amenability of the tested material for supporting the real loading parameters of the component for which the material is intended to be used, mainly in the situations of components and structures of which lifetime duration could be critical influenced by the cracks that are caused by fatigue phenomena. During a single test, the Instron FastTrack d*a*/d*N* Experimental Program is conducting a fatigue test, by loading and unloading the specimen, leading to crack propagation, starting from the tip of a notch that was mechanically processed on the specimen.

## Experimental Tests and Results

The present paper is focused on the evaluation of crack propagation rate using two experimental techniques, based on the tensile testing of carbon steel OLC 45 compact specimens.

The first technique is using the Instron FastTrack d*a*/d*N* Software, especially developed for establishing the crack propagation rate, and installed on the controlling computer of the INSTRON 8801 testing machine. The program protocol includes the starting data: specimen dimensions, extensometer position (gauge location, knife edge thickness, and gauge length –

usually 10 mm), together with some pre-determined material characteristics values (tensile strength, yield strength, Young's modulus, and Poisson's coefficient). The measure of v (opening displacement of crack edges) is automatically supplied by the extensometer on the specimen frontal surface (COD – crack opening displacement); the applied load value is displayed by the computer software, as presented in Figure 7.

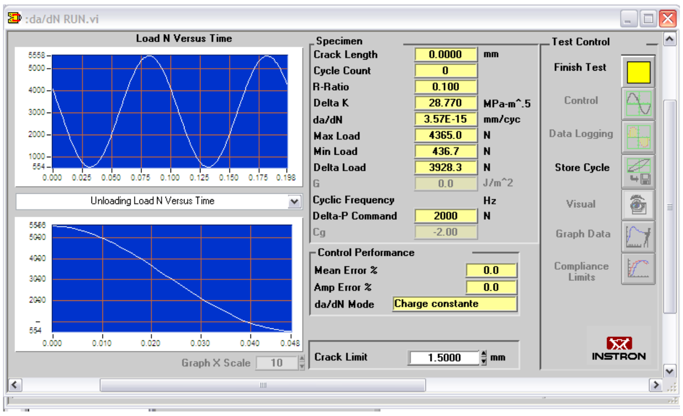

Specimen
Crack Length 0.0000 mm
Cycle Count 0
R-Ratio 0.100
Delta K 28.770 MPa-m^.5
da/dN 3.57E-15 mm/cyc
Max Load 4365.0 N
Min Load 436.7 N
Delta Load 3928.3 N
G 0.0 J/m^2
Cyclic Frequency Hz
Delta-P Command 2000 N
Cg -2.00

Control Performance
Mean Error % 0.0
Amp Error % 0.0
da/dN Mode Charge constante

Crack Limit 1.5000 mm

Graph X Scale 10

**Fig. 7.** A screen capture during the test.

During every experiment, a screen as in the figure is displayed by the computer, allowing for some testing parameters to be chosen: minimum and maximum loading force, limit value of crack length (at which the test will be stopped), frequency of loading force variation.

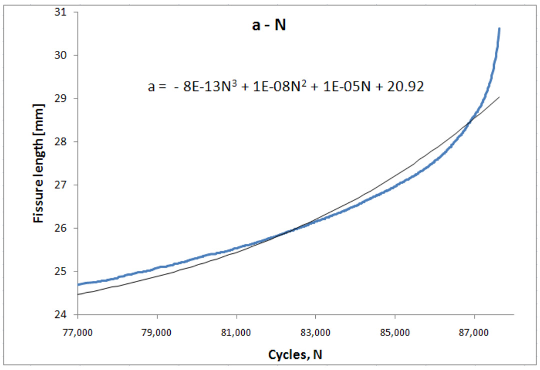

**Fig. 8.** The crack growth with cycles number N

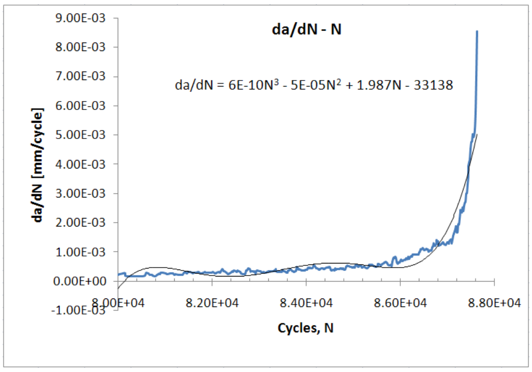

**Fig. 9.** The rate d*a*/d*N* variation with cycles number *N*

The tests results may be presented in data tables, or as variation graphs, which could refer to the dependence on loading cycle's number of one the following experimental parameter: crack length (fig. 8), crack length variation rate (d*a*/d*N*) (fig. 9), stress intensity factor (Δ*K*) (fig. 11). The variation of the rate (d*a*/d*N*) could also be presented, as a function of the last cited factor (Δ*K*) (fig. 10), when it is necessary.

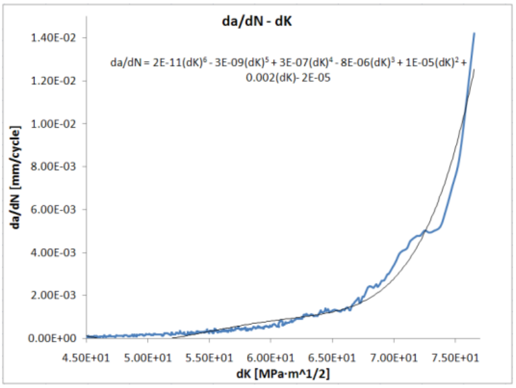

**Fig. 10.** The rate d*a*/d*N* variation with Δ*K*.

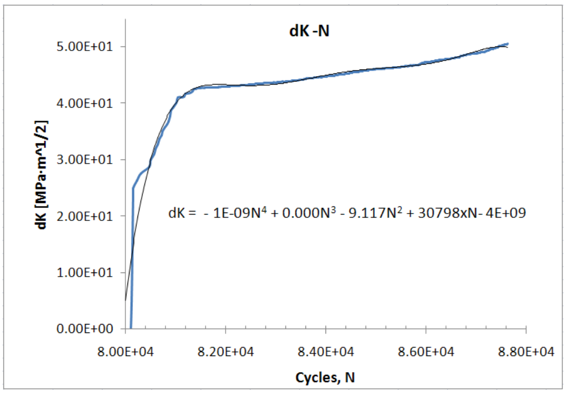

**Fig. 11.** Δ*K* variation with cycles number *N*.

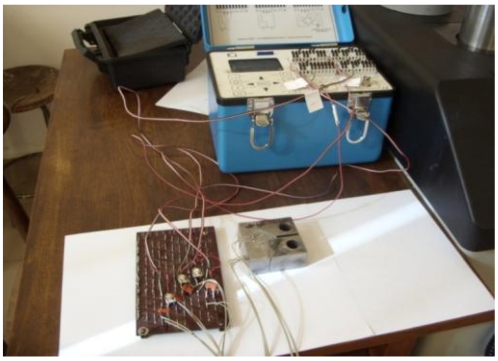

**Fig. 12.** Specimen instrumentation.

The second experimental technique is using the testing data from the above-described crack propagation gage, especially designed for these kinds of tests; it is electrically connected (see figure 12) with the Wheatstone bridge (supplied by Vishay, as the transducers), which is using a data-acquisition card, and is functioning as the power source of the circuit; a supplementary variable electric resistance is also included, for monitoring the output signal of the bridge. The testing data are collected at every second, and so the time data could be converted in loading cycle's number, on the basis of the loading frequency (that is indicated by the testing machine).

After the initial crack propagation (by a fatigue test), into the tested OLC45 carbon steel compact specimen, the crack propagation gage is bonded on the specimen surface, very close to the crack tip. The compact specimen is then loaded in a tensile test (fig. 13), and the crack length tends to extend, including through the transducer (fig. 14), leading to the successively breaking of its elementary filaments.

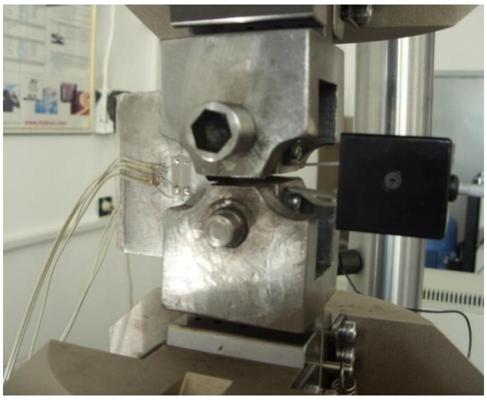

**Fig. 13.** Tensile testing of the compact specimen.

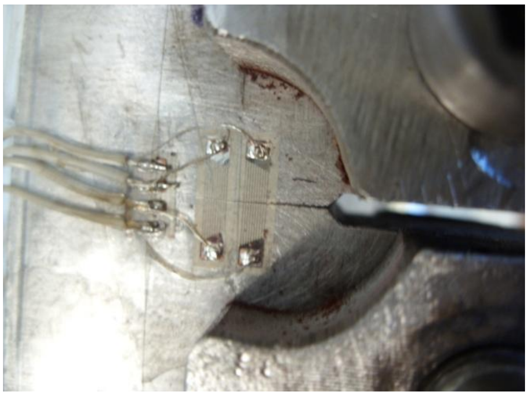

**Fig. 14.** Crack extension in the compact specimen.

The graph from Figure 15 was drawn using the testing data from the Wheatstone bridge: the variation of its output signal is presented, as a function of loading cycle's number; the proper signal is obtained as $\mu\varepsilon$, but it could be converted in mm, by correlating it with the crack length increase. A jump could be observed into the cited graph, every time a single transducer filament is broken, as it was indicated by the transducer supplier (see again figure 3).

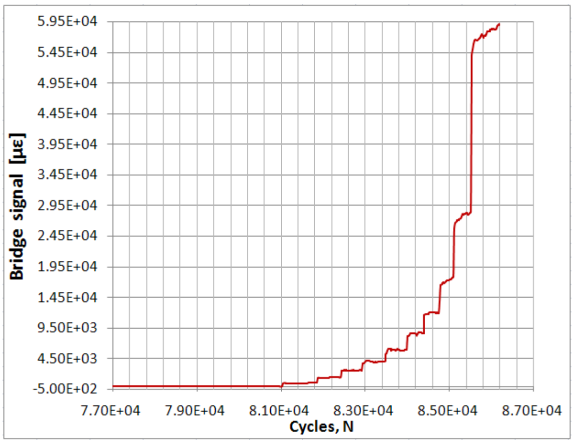

**Fig. 15.** Bridge signal variation with loading cycles number.

The zero value of the crack length is considered when the crack reaches the level of the first crack propagation gage filament; the effective step-distance between the filaments (0.25 mm) is also important for establishing an instant value of the crack length: a correlation is made, between the bridge signal and the crack length increase, from the moment of the first filament breakage. On that basis, the crack growth variation is presented in Figure 16, in dependence with the loading cycle's number (starting with the moment of the first filament breakage). The graph based on the bridge signal can be presented as a continuous line, using the trend line of the signal variation graph.

On the other hand, using the acquisition data from the clip-on-gage transducer, together with some of the above-presented calculus relationship, a data file is supplied, by the computer of the testing machine, and it could be used for building another graph (also drawn in Figure 16); it is approximated by a trend line, described by a 4th degree polynomial equation.

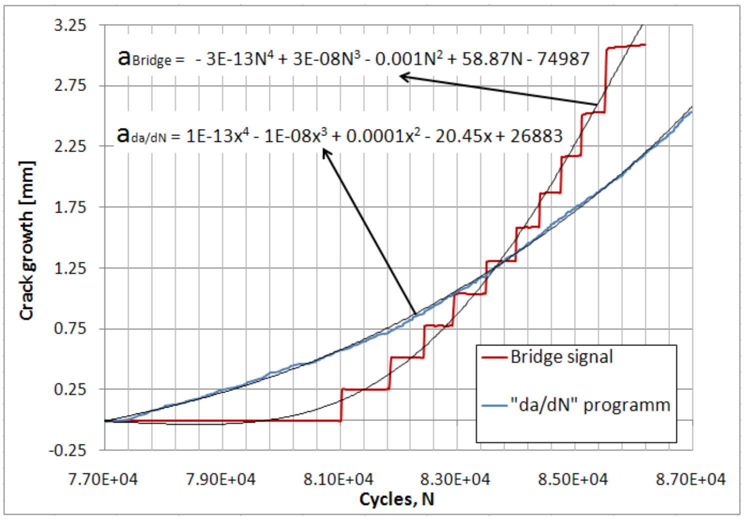

**Fig. 16.** Crack growth as a function of cycles number, using the bridge signal, and respectively the d*a*/d*N* program.

One can say that, although the trend lines of the two graphs are quite different, the values that are given, for the crack growth, by the two expressions are comparable. As a consequence, the above presented experimental techniques could be both assumed as reliable, in order to establish the crack length variation, in dependence with loading cycles number. The advantage, for the method based on the crack propagation gage, is the possibility of being applied on real components, even situated in their working process, by using a wireless transmission of acquisition data at the monitoring center of the experimental program.

## Conclusion

The cyclic loading that plastically deforms a metallic specimen can lead to continuous changes into the material structure. Two different experimental techniques were used, both based on tensile testing of the compact steel specimen, in order to establish the evolution of a crack growth, in dependence with the loading cycles number. The first method uses specialized software on the testing machine computer, collecting data from a clip-on-gage extensometer bonded on the specimen. The second technique uses experimental data from a crack propagation gage, especially designed for measuring the crack growth. A good similarity was observed, between the variation graphs given by the two methods.

The crack propagation gage method may be used for various metallic components and structures, in order to estimate their lifetime duration, when they are susceptible to develop some cracks in their structure [15].

## References

1. Fajdiga G., Sraml M. – Fatigue crack initiation and propagation under cyclic contact loading, *Engineering Fracture Mechanics*, **76**, 2009, pp. 1320–1335.
2. Correia J., De Jesus A., Fernández-Canteli A. – Local unified probabilistic model for fatigue crack initiation and propagation: Application to a notched geometry, *Engineering Structures*, **52**, 2013, pp. 394–407.
3. Beden S.M., Abdullah S., Ariffin A.K. – Review of Fatigue Crack Propagation Models for Metallic Components, *European Journal of Scientific Research*, **28**, 2009, pp. 364-397.
4. Ritchie R.O. – Mechanisms of fatigue-crack propagation in ductile and brittle solids, *International Journal of Fracture*, **100**, 1999, pp. 55-83.
5. Paris P., Erdogan F. – A critical analysis of crack propagation laws, *Journal of Basic Engineering, Transactions of the American Society of Mechanical Engineers*, 1963, pp. 528-534.
6. Donahue, R.J., et al. – Crack opening displacement and the rate of fatigue crack growth, *Int. J. Fract. Mech.*, **8**, 1972, pp. 209–219.
7. Klesnil M., Lukas P. – Influence of strength and stress history on growth and stabilization of fatigue cracks, *Eng. Fract. Mech.*, **4**, 1972, pp. 77–92.
8. Chikwembani S., Weertman J. – Fatigue Crack Growth and Fracture Behavior of Bismuth-Doped Copper Bicrystals, *Metallurgical Transactions A*, 20A, 1989, pp. 1221-1231.
9. Gasem Z., Gangloff R.P. – Rate-limiting processes in environmental fatigue crack propagation in 7000-series aluminum alloys, *Chemistry and Electrochemistry of Corrosion and Stress Corrosion Cracking*, Warrendale, P.A.: TMS-AIME, 2001, pp. 501-521.
10. Erdogan F, Ratwani M. – Fatigue and fracture of cylindrical shells containing circumferential crack, *Int. J. Frac. Mech.*, **4**, 1970, pp. 379-392.
11. Kotowsky M.P. – *Wireless Sensor Networks for Monitoring Cracks in Structures*, Northwestern University, Evanston, Illinois, 2010.
12. * * * – Vishay Micro-Measurements, *Crack Propagation Patterns, Special Use Sensors - Crack Propagation Sensors*, pp. 137-139.
13. * * * – Data book Vishay, *Catalog 500*, Vishay Intertechnology, Inc.
14. * * * – *Instron FastTrack Software da/dN Crack Propagation Program*, Reference Manual - Software, M22-10007-EN, Revision F.
15. * * * – ASTM E647 - 13ae1, *Standard Test Method for Measurement of Fatigue Crack Growth Rates*.

# Utilizarea a două metode experimentale pentru stabilirea variaţiei lungimii fisurii în raport cu numărul ciclurilor de solicitare

## Rezumat

*În lucrare sunt aplicate două metode de determinare a variaţiei lungimii fisurii în raport cu numărul ciclurilor de solicitare. Ambele se bazează pe încercarea la tracţiune a probei compacte din OLC45, tratat termic prin călire. Prima metodă utilizează softul specializat pentru determinarea vitezei de propagare a fisurii, care este instalat pe PC-ul ce controlează maşina de încercat. La rândul lui, acest soft colectează date atât de la maşina de încercat, cât şi de la extensometrul de tip „clip-on-gage” ataşat probei compacte. A doua metodă utilizează date preluate de la un senzor rezistiv special, de tip Vishay (Tk-09-CPB02-005/DP), destinat să determine propagarea fisurii şi lipit în imediata vecinătate a fisurii induse iniţial prin oboseală. Pe baza datelor obţinute se face o comparaţie între cele două metode de determinare, ultima având avantajul că poate fi aplicată chiar la locul de funcţionare a piesei pentru care se stabileşte viteza de propagare a fisurii.*